JOURNAL OF COMPUTATIONAL PHYSICS 70, 311–329 (1987)

Computing Multigroup Radiation Integrals Using Polylogarithm-Based Methods

BRADLEY A. CLARK

Radiation Transport Group, Los Alamos National Laboratory, Los Alamos, New Mexico 87545

Received April 11, 1986; revised September 10, 1986

A new method is derived that is effective in calculating multigroup radiation integrals, i.e., the multigroup Planck spectrum and its derivatives with respect to temperature. This new, polylogarithm-based, method is actually a set of methods that can be made arbitrarily accurate. The accuracy and speed of the new methods are compared with three methods based on: a rational polynomial fit, interpolation in tabular data, and a simple numerical integration scheme. The polylogarithm-based methods are unsurpassed in accuracy, and their execution speed is competitive with the fastest methods tested. In addition, the multigroup integrals that are calculated using the new methods have some desirable properties—proper normalization, positivity, and continuity—that do not all exist in any one of the other methods. © 1987 Academic Press, Inc.

I. INTRODUCTION

A blackbody emits radiation with a frequency spectrum that is characterized by the Planck distribution function. For many thermal-radiation-transport calculations, continuous spectra are approximated by a discrete, multigroup (or multifrequency) spectrum. In that case, the multigroup emission spectrum is characterized by definite integrals of the Planck spectrum over each multigroup frequency interval [1]. Some codes also make use of derivatives of the Planck distribution with respect to temperature. This paper describes a technique that accurately computes these multigroup distributions for an arbitrary set of frequency boundaries.

The remainder of this paper is organized in four sections. Section II presents consistent definitions of the radiation spectra in two typical notations, describes how the analytic integrals are obtained, and shows how they are modified into a useful form. Section III uses the results from Section II to produce a family of efficient numerical methods. Section IV describes the accuracy of the methods and compares the accuracy and computing speed of the new methods with a simple numerical-integration technique. Finally, Section V presents the conclusions.

II. INCOMPLETE INTEGRALS OF THE RADIATION SPECTRA

This section begins with a brief introduction to the Planck spectrum, and its derivatives, written in two typical notations. Symbolic-algebra software is used to

0021-9991/87 $3.00

obtain indefinite integrals of the normalized radiation spectra. The analytic expressions for the Planck integral and its derivatives are rearranged so that they can be accurately evaluated. The final subsection is devoted to obtaining approximate integrals in the low-frequency (or high-temperature) limit.

A. *Definitions—The Planck Spectrum and Its Derivatives*

The Planck radiation spectrum, $B_1(\nu', T)$, describes the distribution of the radiation intensity for a blackbody in thermodynamic equilibrium

$$B_1(\nu', T)\, d\nu' = \frac{2h}{c^2} \frac{\nu'^3}{e^{h\nu'/kT} - 1}\, d\nu', \tag{1}$$

where T is the material temperature, h is Planck's constant, c is the speed of light, ν' is the photon frequency ($\sec^{-1}$), and k is Boltzmann's constant. The Planck spectrum also describes the emission of radiation under the assumption of local thermodynamic equilibrium (LTE).

The Planck spectrum can also be written with the frequency expressed in temperature units; $\nu = h\nu'/k$ and

$$B_2(\nu, T)\, d\nu = \frac{2k^4}{c^2h^3} \frac{\nu^3}{e^{\nu/T} - 1}\, d\nu. \tag{2}$$

Introducing the reduced-frequency variable, $x = h\nu'/kT = \nu/T$, both forms of the Planck spectrum are conveniently written in terms of the normalized Planck spectrum, $b(x)$,

$$B_1(\nu', T)\, d\nu' = B_2(\nu, T)\, d\nu = \frac{\sigma T^4}{\pi} b(x)\, dx, \tag{3}$$

where σ is the Stefan–Boltzmann constant. The normalized Planck spectrum, $b(x)$, is defined by

$$b(x)\, dx = \frac{15}{\pi^4} \frac{x^3}{e^x - 1}\, dx, \tag{4}$$

with the normalization condition

$$\int_0^\infty b(x)\, dx = 1. \tag{5}$$

Derivatives of the multigroup Planck spectrum with respect to temperature are sometimes useful in numerical solutions and analysis. The first derivative, also called the Rosseland function, is useful when the Planck spectrum is linearized using a first-order Taylor-series expansion. Both the first and second derivatives can be useful in analyzing the stability and accuracy of such linearizations.

The Rosseland spectrum can be written in two analogous forms, each is the derivative with respect to temperature of the corresponding Planck spectrum

$$R_1(\nu', T)\,d\nu' = \frac{\partial B_1(\nu', T)}{\partial T}\,d\nu' = \frac{2h^2}{c^2kT^2}\,\frac{\nu'^4 e^{h\nu'/kT}}{(e^{h\nu'/kT}-1)^2}\,d\nu', \tag{6a}$$

and

$$R_2(\nu, T)\,d\nu = \frac{\partial B_2(\nu, T)}{\partial T}\,d\nu = \frac{2k^4}{c^2h^3T^2}\,\frac{\nu^4 e^{\nu/T}}{(e^{\nu/T}-1)^2}\,d\nu. \tag{6b}$$

Utilizing the reduced frequency, $x = h\nu/kT$, the Rosseland spectra are written in terms of the normalized Rosseland spectrum, $r(x)$,

$$R_1(\nu', T)\,d\nu' = R_2(\nu, T)\,d\nu = \frac{4\sigma T^3}{\pi}\,r(x)\,dx, \tag{7}$$

where

$$r(x)\,dx = \frac{15}{4\pi^4}\,\frac{x^4 e^x}{(e^x-1)^2}\,dx, \tag{8}$$

with the normalization condition

$$\int_0^\infty r(x)\,dx = 1. \tag{9}$$

The second-derivative spectrum can be written in the same two forms, each being the second derivative of the Planck function with respect to temperature

$$\begin{aligned} S_1(\nu', T)\,d\nu' &= \frac{\partial^2 B_1(\nu', T)}{\partial T^2}\,d\nu' \\ &= \frac{2h^2}{c^2kT^3}\,\frac{\nu'^4 e^{h\nu'/kT}}{(e^{h\nu'/kT}-1)^3}\left[2 + \frac{h\nu'}{kT} + e^{h\nu'/kT}\left(\frac{h\nu'}{kT} - 2\right)\right]d\nu' \end{aligned} \tag{10a}$$

and

$$\begin{aligned} S_2(\nu, T)\,d\nu &= \frac{\partial^2 B_2(\nu, T)}{\partial T^2}\,d\nu \\ &= \frac{2k^4}{c^2h^3T^3}\,\frac{\nu^4 e^{h\nu/kT}}{(e^{h\nu/kT}-1)^3}\left[2 + \frac{\nu}{T} + e^{\nu/T}\left(\frac{\nu}{T} - 2\right)\right]d\nu. \end{aligned} \tag{10b}$$

The normalized second-derivative spectrum is defined such that

$$S_1(\nu', T)\,d\nu' = S_2(\nu, T)\,d\nu = \frac{12\sigma T^2}{\pi}\,s(x)\,dx, \tag{11}$$

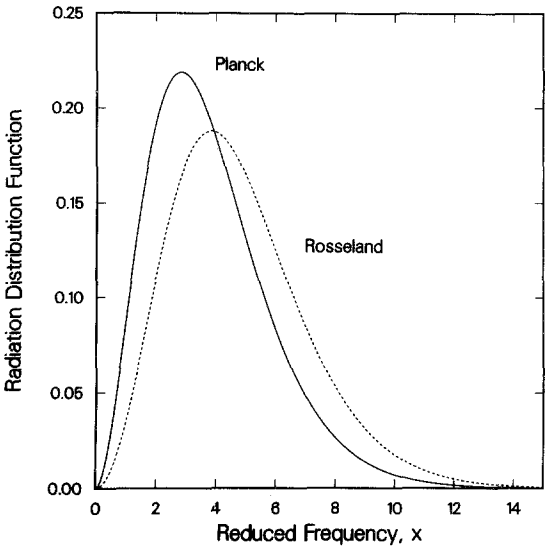

FIG. 1. Normalized Planck and Rosseland spectra.

where

$$s(x)\,dx = \frac{15}{12\pi^4}\,\frac{x^4 e^x[2+x+e^x(x-2)]}{(e^x-1)^3}\,dx, \tag{12}$$

with the normalization condition

$$\int_0^\infty s(x)\,dx = 1. \tag{13}$$

The normalized spectra—$b(x)$, $r(x)$, and $s(x)$—are convenient because they contain all of the frequency dependence and are independent of temperature. Thus, the right-hand expressions in Eqs. (3), (7), and (13) are separated into the product of temperature-dependent and frequency-dependent terms. The normalized Planck and Rosseland spectra, $b(x)$ and $r(x)$, are shown in Fig. 1.

B. *Incomplete Integrals of the Radiation Spectra*

The indefinite integrals of the normalized Planck, Rosseland, and second-derivative spectra, defined in Eqs. (4), (8), and (12), respectively, are obtained using the MACSYMA symbolic algebra software[1]

[1] The Mathlab Group, Laboratory for Computer Science, Massachusetts Institute of Technology, MACSYMA Reference Manual, Version 10 (Symbolics, Inc., Cambridge, Ma., 1983). MACSYMA is a large symbolic manipulation program developed at the MIT Laboratory for Computer Science and supported from 1975–1983 by the National Aeronautics and Space Administration under Grant NSG-1323, by the Office of Naval Research under Grant N00014-77-C-0641, by the U.S. Department of Energy under Grant ET-78-C-02-4687, and the U.S. Air Force under Grant F49620-79-C-020, and since 1982 by Symbolics, Inc. of Cambridge, Ma. MACSYMA is a trademark of Symbolics, Inc.

$$\int b(x)\,dx = \frac{15}{\pi^4}\left[6Li_4(e^x) - 6xLi_3(e^x) + 3x^2Li_2(e^x) + x^3\log(1-e^x) - \frac{x^4}{4}\right] + C_1, \tag{14}$$

$$\int r(x)\,dx = \frac{15}{\pi^4}\left[6Li_4(e^x) - 6xL_3(e^x) + 3x^2Li_2(e^x) + x^3\log(1-e^x) - \frac{x^4}{4} - \frac{x^4}{4(e^x-1)}\right] + C_2 \tag{15}$$

and

$$\int s(x)\,dx = \frac{15}{\pi^4}\left[6Li_4(e^x) - 6xLi_3(e^x) + 3x^2Li_2(e^x) + x^3\log(1-e^x) - \frac{x^4}{4} - \frac{x^4(xe^x-3)}{12(e^x-1)^2}\right] + C_3, \tag{16}$$

where $Li_n(z)$ is the general polylogarithm function, discussed in depth by Lewin [2]. The integration constants, C_1, C_2, and C_3, are defined subsequently. To the author's knowledge, Eqs. (14)–(16) are new results; they are not found in any table of integrals.

A brief description of polylogarithms follows, it includes only the information that is needed for clarity; more-detailed information is available from Lewin [2] and the references cited therein. Polygarithms are complex functions defined recursively for complex z,

$$Li_n(z) = \int_0^z \frac{Li_{n-1}(z')}{z'}\,dz' \tag{17}$$

for $n > 2$. The recursion begins with the relatively well-known dilogarithm, $Li_2(z)$,

$$Li_2(z) = -\int_0^z \frac{\log(1-z')}{z'}\,dz'. \tag{18}$$

Polylogarithms can be evaluated using the series

$$Li_n(z) = \sum_{l=1}^{\infty} \frac{z^l}{l^n}, \tag{19}$$

provided $|z| \leqslant 1$. For the radiation integrals, x is real and $0 \leqslant x \leqslant \infty$; thus $1 \leqslant e^x \leqslant \infty$. Therefore, because the polylogarithm's arguments are outside the range of convergence, the polylogarithms in Eqs. (14), (15), and (16) cannot be directly evaluated using Eq. (19). In view of this complication, it would seem that the

analytic integrals are of little value for practical calculations. However, Kölbig *et al.* [3], presented the argument-inversion relation for polylogarithms

$$Li_n(z)+(-1)^n Li_n(1/z)=-\frac{(2\pi i)^n}{n!}\beta_n\left(\frac{\log z}{2\pi i}\right), \tag{20}$$

where $\beta_n(z)$ is the Bernoulli polynomial [4] of order n, and $i=\sqrt{-1}$. Using Eq. (20), argument-inversion relations are obtained for polylogarithms of orders $2-4$ in the specific case of real exponential arguments

$$Li_2(e^x)+Li_2(e^{-x})=-\frac{x^2}{2}-i\pi x+\frac{\pi^2}{3}, \tag{21a}$$

$$Li_3(e^x)-Li_3(e^{-x})=-\frac{x^3}{6}-\frac{i\pi x^2}{2}+\frac{\pi^2 x}{3}, \tag{21b}$$

and

$$Li_4(e^x)+Li_4(e^{-x})=-\frac{x^4}{24}-\frac{i\pi x^3}{6}+\frac{\pi^2 x^2}{6}+\frac{\pi^4}{45}. \tag{21c}$$

Using Eqs. (21), the polylogarithms in Eq. (14) can be rewritten in terms of polylogarithms with arguments of the form e^{-x}. This inversion of the arguments gives rise to imaginary terms that can be neglected because $b(x)$ is a real function, so $\int b(x)\,dx$ must also be real. Define the incomplete Planck radiation integral, Π where

$$\Pi(x)\equiv\int_0^x b(x')\,dx', \tag{22}$$

which can be written in terms of the polylogarithm functions as

$$\Pi(x)=\frac{15}{\pi^4}\left[-6Li_4(e^{-x})-6xLi_3(e^{-x})-3x^2Li_2(e^{-x})+x^3\log(e^x-1)-x^4\right]+1. \tag{23}$$

The integration constant C_1 is chosen to be -1 so that $\Pi(0)=0$; clearly then, $\Pi(\infty)=1$.

The logarithmic term in Eq. (23) can be simplified to reduce roundoff error at large x by making use of the identity

$$-x^4+x^3\log(e^x-1)=x^3\log(1-e^{-x}); \tag{24}$$

thus,

$$\Pi(x)=\frac{15}{\pi^4}\left[-6Li_4(e^{-x})-6xLi_3(e^{-x})-3x^2Li_2(e^{-x})+x^3\log(1-e^{-x})\right]+1. \tag{25}$$

The incomplete Rosseland radiation integral, Υ, is defined as

$$\Upsilon(x) \equiv \int_0^x r(x')\,dx'. \tag{26}$$

From Eqs. (14) and (15), Υ can be written in terms of Π as

$$\Upsilon(x) = \Pi(x) - \frac{15}{4\pi^4}\frac{x^4}{e^x - 1}, \tag{27}$$

where $C_2 = -1$ is chosen so that $\Upsilon(0) = 0$. Thus, from Eq. (27), if Π is known then Υ is easily obtained without any further approximation.

Similarly, the incomplete second-derivative integral, Δ, is defined as

$$\Delta(x) \equiv \int_0^x s(x')\,dx', \tag{28}$$

which is related to Π as

$$\Delta(x) = \Pi(x) - \frac{15}{12x^4}\frac{x^4[e^x(x+3) - 3]}{(e^x - 1)^2}, \tag{29}$$

where $C_3 = -1$ is chosen so that $\Delta(0) = 0$.

From the normalization conditions, Eqs. (5), (9), and (13), it is apparent that

$$\lim_{x \to \infty} \Pi(x) = \lim_{x \to \infty} \Upsilon(x) = \lim_{x \to \infty} \Delta(x) = 1. \tag{30}$$

The polylogarithm functions in Eq. (25) are readily evaluated using the power-series in Eq. (19). The series converges for all relevant values of x and accurately computes Π, Υ, and Δ if enough terms are used. However, because the series converges slowly as $e^{-x} \to 1$, better computational efficiency is achieved with specialized methods as $x \to 0$.

Equations (27) and (29) indicate that the integrals of both of the derivative spectra are analytically related to Π. Thus, no additional numerical techniques are necessary to evaluate the derivative spectra. Once Π is calculated, the integrals of the derivative spectra—Υ and Δ—can be obtained with very little extra effort, and without any further approximation.

C. *Incomplete Integrals in the Small-x Limit*

The normalized Planck spectrum, $b(x)$, is expanded in a Taylor series in x,

$$b(x) = \frac{15}{\pi^4}\left[x^2 - \frac{x^3}{2} + \frac{x^4}{12} - \frac{x^6}{720} + \frac{x^8}{30240} - \frac{x^{10}}{1209600} + \frac{x^{12}}{47900160} - \cdots\right]. \tag{31}$$

The series representation of $b(x)$ is substituted into Eq. (22) and integrated term-by-term to obtain an infinite-series representation for $\Pi(x)$ which converges rapidly

for small x. If terms in the integrated series that include powers of x greater than x^N are truncated, the resulting finite series, $\tilde{\Pi}_N(x)$, approximates Π with some truncation error. For example, when $N=13$,

$$\tilde{\Pi}_{13}(x)=\frac{15}{\pi^4}\left[\frac{x^3}{3}-\frac{x^4}{8}+\frac{x^5}{60}-\frac{x^7}{5040}+\frac{x^9}{272160}-\frac{x^{11}}{13305600}+\frac{x^{13}}{622702080}\right]. \quad (32)$$

The integration constant is chosen so that $\tilde{\Pi}_N(0)=0$. The truncation error is $\tilde{E}_N(x)$, where

$$\tilde{E}_N(x)=\tilde{\Pi}_N(x)-\Pi(x). \quad (33)$$

$\tilde{\Pi}_N(x)$ and $\Pi(x)$ do not approach the same limit as $x\to\infty$. In particular,

$$\lim_{x\to\infty}\tilde{\Pi}_N(x)=+\infty \qquad \text{for} \quad N=3, 5, 9, 13, 17,... \quad (34a)$$

and

$$\lim_{x\to\infty}\tilde{\Pi}_N(x)=-\infty \qquad \text{for} \quad N=4, 7, 11, 15,.... \quad (34b)$$

Equation (34a) describes the behavior of the truncated series with positive truncation error (PTE) and Eq. (34b) describes the behavior of series with negative truncation error (NTE). Either type of series is accurate within a particular range of x. However, the behavior of these functions in the limit as $x\to\infty$ has implications on their usefulness in conjunction with Eq. (25) that are discussed in the next section.

III. Numerical Methods

This section describes how the series representations of the incomplete radiation integrals are used to efficiently obtain accurate multigroup integrals in a computationally efficient manner. The truncation errors in the polylogarithm and Taylor series are examined numerically. Then, using each type of series where it is most-rapidly convergent, a family of methods is obtained for efficiently evaluating the incomplete radiation integrals.

The objective of the numerical methods is to accurately compute b_g from an approximate evaluation of Π. The incomplete radiation integral, $\Pi(x)$, can be used to calculate the definite integrals of the radiation spectra as

$$b_g=\int_{x_g}^{x_{g+1}} b(x')\,dx'=\Pi(x_{g+1})-\Pi(x_g). \quad (35)$$

Care must be taken in evaluating Eq. (35) to ensure that roundoff errors do not contaminate the subtraction.

A. *Calculating* II

$\Pi(x)$ is the incomplete integral of the Planck spectrum, see Eq. (25); it is expressed in terms of polylogarithms that can be evaluated with an infinite series, Eq. (19). It is efficient to evaluate the logarithmic term in Eq. (25) using a similar series,

$$\log(1+z)=\sum_{k=1}^{\infty}(-1)^{k+1}\frac{z^k}{k} \tag{36}$$

if $-1<z\leqslant 1$. Therefore,

$$\log(1-e^{-x})=-\sum_{k=1}^{\infty}\frac{e^{-kx}}{k}. \tag{37}$$

Although the strict inequality for Eq. (36) is violated when $x=0$ and $-e^{-x}=-1$, it will be shown later that this series will not be used in that limit. [It is interesting to note that the series in Eq. (37) is exactly that which would be obtained from Eq. (19) for $Li_1(e^{-x})$ if $Li_1$was defined.]

Substituting the series representations of $Li_n(e^{-x})$ and $\log(1-e^{-x})$ from Eqs. (19) and (37) into Eq. (25) and truncating each series to L terms, yields Π_L, a series approximation to $\Pi(x)$,

$$\Pi_L(x)=1+\frac{15}{\pi^4}\left[-x^3\sum_{l=1}^{L}\frac{e^{-lx}}{l}-3x^2\sum_{l=1}^{L}\frac{e^{-lx}}{l^2}-6x\sum_{l=1}^{L}\frac{e^{-lx}}{l^3}-6\sum_{l=1}^{L}\frac{e^{-lx}}{l^4}\right]. \tag{38}$$

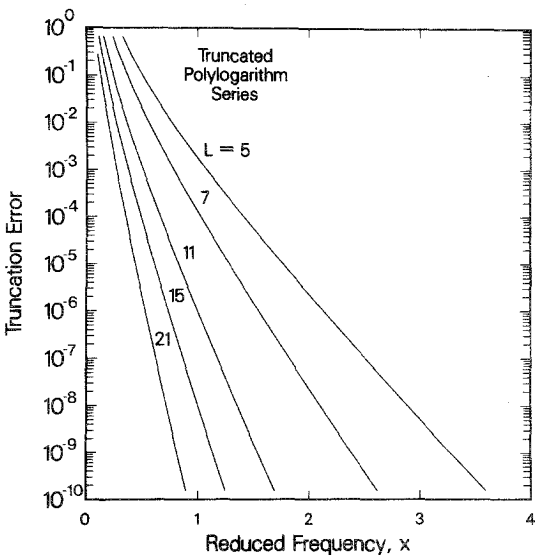

FIG. 2. Relative truncation error in the polylogarithm expansion.

The truncation error, $E_L(x)$, is

$$E_L(x) = \Pi_L(x) - \Pi(x), \tag{39}$$

where $\Pi(x)$ is the exact integral.

The series in Eq. (38) converge rapidly in l when x is large due to the e^{-lx} dependence; however, as $x \to 0$ the series converge slowly. Figure 2 illustrates the relative error, $E_L(x)/\Pi(x)$, as a function of x for a few typical values of L.

The curves in Fig. 2 demonstrate the rapid convergence of the series in Eq. (38) for the larger x values, e.g., seven terms reduce the relative error below 10^{-7} for all $x > 2$. However, it is also evident that many more terms are required as $x \to 0$. This slow convergence illustrates the need for alternate methods for evaluating Π as $x \to 0$. To be useful, the candidate method must be more efficient than simply evaluating Eq. (38) with larger L.

B. *Calculating* $\tilde{\Pi}_N$

Equation (32) approximates $\tilde{\Pi}(x)$ and is obtained by integrating the truncated Taylor series expansion of $b(x)$. Figure 3 shows the relative truncation error, $\tilde{E}_N(x)/\Pi(x)$ [see Eq. (32)], plotted along with $E_L(x)/\Pi(x)$; it illustrates the rapid convergence of the integrated Taylor series in the limit as $x \to 0$. Figure 3 also shows that a combination of Π_L and $\tilde{\Pi}_N(x)$ can accurately approximate $\Pi(x)$ if an appropriate number of terms are summed in each series. For example, to ensure that the relative error in Π is less than 10^{-5}, various combinations of L and N could be chosen; specifically, $L = 7$ and $N = 9$, or $L = 15$ and $N = 9$, or $L = 5$ and $N = 13$ would all meet that criterion. Using different combinations of truncation

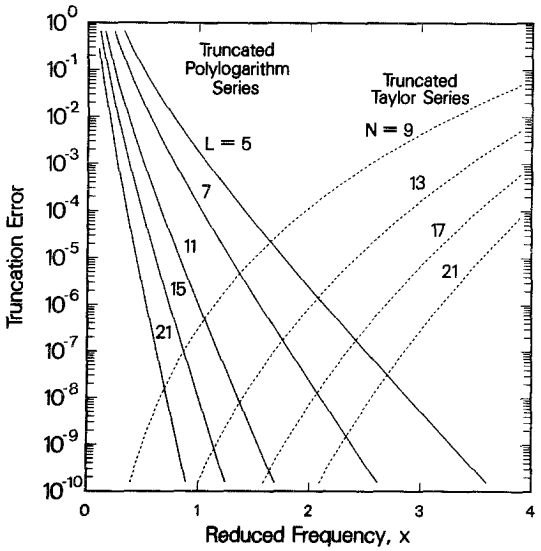

FIG. 3. Relative truncation error of the series expansions.

parameters in the two series produces different approximations to the radiation integral with different accuracy and computational speed.

C. *Combining the Approximation to* Π

In discussing combined-series methods for approximating $\Pi(x)$, it is useful to locate the point where the two series are equal. This point, ζ, is defined by the continuity condition

$$\Pi_L(\zeta) = \tilde{\Pi}_N(\zeta). \tag{40}$$

ζ is a nonlinear function of L and N and can only be obtained numerically. However, there is no guarantee that a solution for ζ will exist for every L, N pair.

Figure 4 shows $\Pi(x)$ and several approximations to $\Pi(x)$; the difference between $\Pi(x)$ and the approximations has been magnified by a factor of 100 for the sake of discussions. Specifically, the curve marked Π_5 is really $\Pi(x) + 100E_5(x)$ and $\tilde{\Pi}_9$ is really $\Pi(x) + 100\tilde{E}_9(x)$. The truncated polylogarithm series, $\Pi_5(x)$, is accurate for $x > 1$ despite using only 5 terms in each polylogarithm series. Figure 4 also shows the dual character of the truncated Taylor series approximations in the large-x limit. As indicated in Section I, when the truncation error is negative [e.g., $\Pi_{11}(x)$], the Taylor-series approximation approaches $-\infty$ for large x. Conversely, if the truncation error is positive [e.g., $\Pi_9(x)$] then the approximate function approaches $+\infty$ for large x.

Figure 5 shows a closer view of the data in Figure 4 in the vicinity of ζ; in this case the errors have been magnified by 1000. $\tilde{\Pi}_{11}(x)$ does not intersect the truncated polylogarithm curve $\Pi_5(x)$, and there is no solution for ζ. However, $\Pi_5(x)$

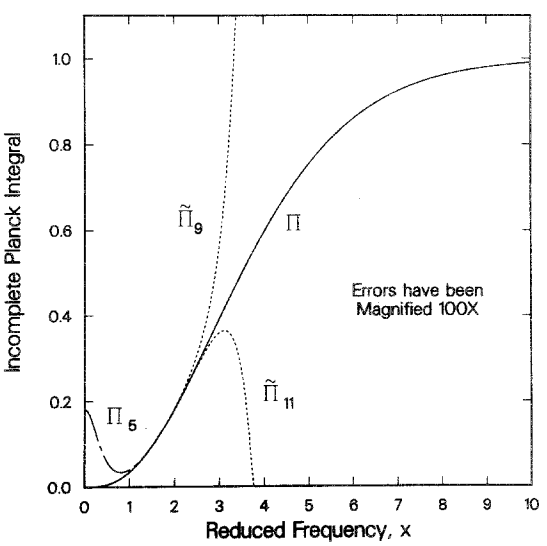

FIG. 4. Π and approximations with magnified errors.

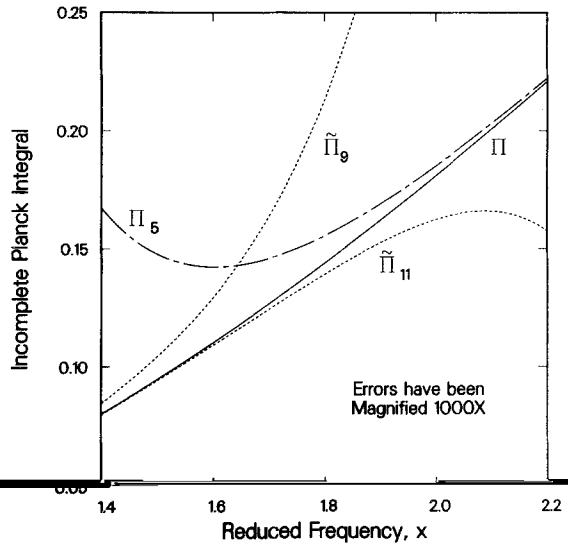

FIG. 5. Π and approximations with magnified errors.

and $\tilde{\Pi}_9(x)$ intersect and a solution for ζ exists. This behavior has been found to be true in general, regardless of the polylogarithm truncation: a solution for ζ exists for truncated Taylor-series expansions with positive truncation error ($N = 3, 5, 9, 13, 17,...$) but ζ does not exist for series with negative truncation error ($N = 4, 7, 11, 15,...$).

The behavior illustrated in Fig. 5 has an important impact on the construction of numerical methods for approximating $\Pi(x)$. First, because ζ does not exist for NTE series, any approximation to $\Pi(x)$ that uses them is necessarily discontinuous. Further, if such a discontinuous approximation is used in Eq. (35), then the calculated b_g will be a discontinuous function of temperature. Second, if a PTE Taylor series is used then an approximate $\Pi(x)$ can be constructed from the minimum of the two approximations, i.e.,

$$\Phi_{N,L}(x) = \min[\Pi_L, \tilde{\Pi}_N(x)]. \tag{41}$$

Due to the discontinuity that arises when the Taylor series with negative truncation error are used, and because Eq. (41) is so simple, henceforth the discussion is restricted to truncated Taylor series with positive truncation error ($N = 3, 5, 9, 13, 17,...$).

As defined in Eq. (41), $\Phi_{N,L}(x)$ is an accurate approximation to the incomplete Planck radiation integral. $\Phi_{N,L}(x)$ is useful in calculating the multigroup cumulative probability distribution [5] for sampling the Planck spectrum in multigroup Monte Carlo codes. Because it retains the same normalization as Π, $\Phi_{N,L}$ is appropriately normalized for sampling, i.e.,

$$\Phi_{N,L}(0) = 0 \tag{42}$$

and

$$\lim_{x \to \infty} \Phi_{N,L}(x) = 1. \tag{43}$$

Utilizing $\Phi_{N,L}(x)$ on the right-hand side of Eq. (35) is an effective method for calculating b_g. However, it does suffer from roundoff error for large x. Recall that for large x, Π approaches 1 and the subtraction in Eq. (35) is between two values close to 1, but their difference, b_g, is many orders of magnitude smaller. Equations (35) and (41) cannot accurately calculate values of b_g smaller than 10^{-15} on the CRAY computers. (In the small-x limit, where $\Pi(x)$ also approaches 0, roundoff error is not a problem.) Although this limitation may not seem to be serious, it is easily remedied.

The roundoff error is eliminated with a slight modification of Eqs. (35) and (41). Introduce an artifical discontinuity in Φ at $x = \zeta$

$$\Gamma_{N,L}(x) = \begin{cases} \tilde{\Pi}_N(x), & \text{if } x < \zeta, \\ \Pi_L(x) - 1, & \text{if } x \geqslant \zeta. \end{cases} \tag{44}$$

When x is large, then $\Gamma_{N,L}(x) = \Pi_L(x) - 1$. However, from Eq. (38), the substraction in $\Pi_L(x) - 1$ can be done algebraically instead of numerically; and because $\lim_{x \to \infty} \Pi_L(x) - 1 = 0$, the roundoff error is eliminated. A typical composite function, $\Gamma_{N,L}(x)$, is shown in Fig. 6.

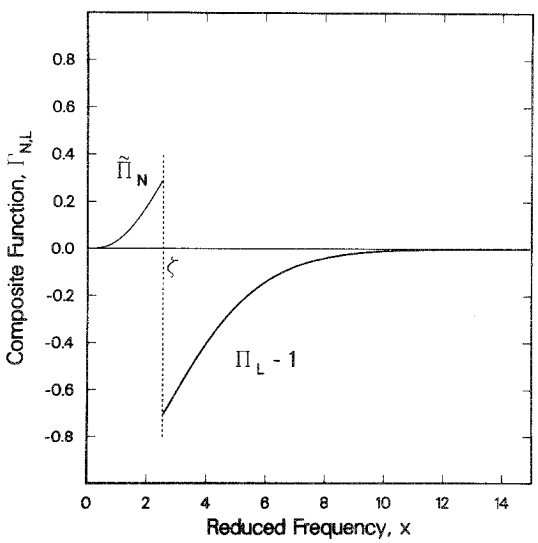

FIG. 6. The composite function $\Gamma_{N,L}$.

Substituting $\Gamma_{N,L}$ for Π in Eq. (35) yields

$$b_g = \begin{cases} \tilde{\Pi}_N(x_{g+1}) - \tilde{\Pi}_N(x_g), & \text{if } x_{g+1} < \zeta \\ \Pi_L(x_{g+1}) - \tilde{\Pi}_N(x_g) - 1, & \text{if } x_g \leqslant \zeta < x_{g+1} \\ \Pi_L(x_{g+1}) - \Pi_L(x_g) & \text{if } x_g \geqslant \zeta. \end{cases} \tag{45}$$

The first and third results are correct from the direct application of Γ to Eq. (35). However, the result that is produced for the group defined by the relation $x_g \leqslant \zeta < x_{g+1}$ is actually $b_g - 1$, which is negative. In fact, this is the only situation that can lead to a negative b_g. The negative value is easily detected and 1 is added to it to obtain the correct result, b_g. Thus, the discontinuity that was introduced in Eq. (44) is removed and b_g remains a continuous function of temperature.

A simple restatement of Eq. (44) allows the entire algorithm to be implemented without explicit knowledge of ζ, i.e.,

$$\Gamma_{N,L}(x) = \begin{cases} \tilde{\Pi}_N(x), & \text{if } \tilde{\Pi}_N(x) > \Pi_L(x) \\ \Pi_L(x) - 1, & \text{if } \tilde{\Pi}_N(x) \leqslant \Pi_L(x). \end{cases} \tag{46}$$

Equation (46) is preferable to Eq. (44) because there is no need to calculate ζ, which can be time-consuming.

IV. Results

The previous sections of this paper defined a family of polylogarithm-based (PB) methods for evaluating the multigroup Planck radiation integrals, and their derivatives. In this section, a simple test problem is used to study the accuracy and computing speed trade-offs for the new methods. The speed and accuracy of the new methods are compared with three methods that are in common use.

A. *Test Problem*

The objective of the methods described herein is to evaluate multigroup radiation integrals. The test problem chosen in representative of the realistic requirements that are placed on the algorithms. The reduced-frequency space is divided into 60 groups spaced logarithmically between 0.1 and 20. Two groups are added to span the entire positive x range; the first group extends from 0 to 0.1 and the last group spans the range from 20 to ∞. Because the timing of routines on the CRAY computers depends on the mode of vectorization, the timing results are compared for 200 "zones" or temperatures.

To evaluate the effectiveness of the methods derived herein, the new methods are compared with three existing techniques that are commonly used to evaluate multigroup Planck integrals. The three other methods are: a modified trapezoid-rule, a rational approximation, and a table look-up method.

The modified trapezoid-rule (MTR) technique uses the integration formula

$$b_g = \frac{15}{\pi^4}(x_{g+1} - x_g)\frac{\langle x\rangle^3}{e^{\langle x\rangle} - 1}, \tag{47}$$

where $\langle x\rangle = \sqrt{x_g x_{g+1}}$. The MTR is chosen for its simplicity and ease of vectorization; it is not expected to be very accurate. However, the MTR should determine an upper bound on the speed of such routines.

The second technique, the rational polynomial fit (RPF), was obtained by Zimmerman [6]. In the RPF method, $\Pi(x_g)$ and $\Pi(x_{g+1})$ are approximated by

$$\Pi(x) = \begin{cases} \tilde{\Pi}_3(x) & \text{if} \quad x_{g+1} < 10^{-3} \\ 1 - \dfrac{15}{\pi^4}\dfrac{a_0 + a_1 x + a_2 x^2 + a_3 x^3 + a_4 x^4 + a_5 x^5}{1 + b_1 x + a_5 x^2} e^{-x} & \text{if} \quad x_{g+1} \geqslant 10^{-3}, \end{cases} \tag{48}$$

where,

$$a_0 = 6.493939402267,$$
$$a_1 = 8.317008834543,$$
$$a_2 = 5.570970415031,$$
$$a_3 = 2.161761553097,$$
$$a_4 = 0.5194172986679,$$
$$a_5 = 0.07713864107538,$$

and

$$b_1 = 0.2807339758744.$$

For the RPF method, the equation used to evaluate $\Pi(x_g)$ depends on the value of x_{g+1}. Therefore, in some instances, the second relation in Eq. (48) is used for values of x that are much less than 10^{-3}. The RPF routine makes use of Eq. (27) to calculate the multigroup Rosseland spectrum. The comments in the RPF routine indicate that the accuracy of the integrals is 0.2%.

The third technique, the table look-up (TLU) method, is a product of the DRAD[2] radiation hydrodynamics code effort. For most values of x, the algorithm performs table look-ups to approximate Π when $1.9 < x \leqslant 12$. Outside of that range, Π is calculated as

$$\Pi(x) = \begin{cases} \tilde{\Pi}_9(x) & \text{if} \quad x \leqslant 1.9 \\ 1 - \dfrac{15}{\pi^4}(6 + 6x + 3x^2 + x^3)\, e^{-x}, & \text{if} \quad x > 12. \end{cases} \tag{49}$$

[2] Theoretical and Computational Radiation Hydrodynamics, Volume II, The DRAD code—Compton Scattering. GA-9530, Vol. II, 1969.

The second case in Eq. (49) is obtained by integrating $b(x)$ in the limit of large x, specifically when $e^x \gg 1$; in that limit, Π can be approximated by $15 \int x^3 e^{-x}\, dx/\pi^4$. The TLU method is not vectorized.

B. *Accuracy*

The polylogarithm-based methods derived in this paper can achieve any desired accuracy by increasing the number of terms in the series expansions in Eq. (46). To bracket the range of accuracy and computing speed, three PB methods are compared with the other methods described in the previous section. The principal measure that is used to compare the accuracy of the methods is the maximum relative error in any b_g. The "correct" results, used to compute these errors, are obtained with a 7-point adaptive Newton–Cotes quadrature rule; these values are correct to within a 10^{-13} relative error criterion. There are other measures of accuracy that will be discussed later, but their importance is secondary.

The first column of data in Table I summarizes the accuracy of the methods tested. The methods are listed roughly in order of decreasing accuracy. This paper does not address the question of an acceptable error; each individual application must determine an appropriate maximum error. An advantage of the PB methods is that they can be tailored to meet almost any accuracy requirement.

The Newton–Cotes numerical integration method (NC7) is clearly the most accurate method tested. However, the most-accurate PB method tested, $\Gamma_{21,10}$, has a maximum relative error that is less than 5×10^{-10}, which is probably more than adequate for most applications. More accurate results can always be obtained by increasing N and L in Eq. (46). Table I indicates the wide range of accuracy (10^{-3} to 10^{-10}) that is achieved using the three PB methods. The RPF and TLU methods are comparable to each other in accuracy ($< 3 \times 10^{-3}$) but both methods are less accurate than the PB methods. These results confirm that the accuracy of the RPF method is bounded by 0.2%.

TABLE I

Planck Integral Methods—Errors and CPU Time

Method	Maximum rel. error[a]	CPU[b] (μsec) Planck only	CPU[b] (μsec) Planck + Rosseland
NC7[c]	1.0×10^{-13}	160	—
$\Gamma_{21,10}$	3.5×10^{-10}	0.95/1.92	1.05/2.08
$\Gamma_{17,5}$	1.2×10^{-6}	0.73/1.47	0.82/1.69
$\Gamma_{9,3}$	1.0×10^{-3}	0.56/1.15	0.67/1.36
RPF	2.2×10^{-3}	—/1.09	—/1.30
TLU	2.5×10^{-3}	6.9	—
MTR	1.0×10^{0}	0.36/0.59	0.41/0.69

[a] $\sup|(b_g - b_g^{\mathrm{NC7}})/b_g^{\mathrm{NC7}}|$.
[b] Group-wise vectorization–zone-wise vectorization.
[c] Newton–Cotes 7-pt. numerical integration.

The MTR method produces results with very large errors. In addition, the MTR method is sensitive to the location of the group boundaries; these errors can be much larger when the temperature is either very large or very small compared to the frequency boundaries. The MTR errors are also sensitive to the spacing between group boundaries.

There are alternate, possibly less-important, measures of the accuracy: proper normalization, and continuity of the approximate Π function. In some situations, these secondary accuracy considerations can impact the maximum relative-error.

When the multigroup integrals are properly normalized, $\sum b_g = 1$. This normalization is hepful in obtaining correct radiation temperatures as the radiation comes into equilibrium with the material. Proper normalization also ensures that the numerical emission by the material agrees with the LTE theory. Renormalization, i.e., adjusting one or all of the b_g values to achieve the proper normalization, can have significant impact on the accuracy of b_g. In particular, if a simple additive correction is performed then the possibility of a negative b_g arises when $\sum b_g > 1$ for the unnormalized spectrum. The MTR method is the only method that yields a significant normalization error. For the MTR, $|1 - \sum b_g| = 2.7 \times 10^{-4}$. Experience has shown that the MTR renormalization error is extremely sensitive to the location and spacing of the multigroup boundaries. For all other methods that were tested, the normalization error is less than 10^{-14}.

Continuity of Π is desirable because when $\partial\Pi/\partial x$ is unbounded, the calculated b_g near the discontinuity becomes a discontinuous function of temperature. A discontinuous variation of b_g to temperature changes can be particularly difficult to deal with when iterative methods are used to solve the transport equation. If $\partial\Pi/\partial x$ remains bounded, as it does for the PB and MTR methods, then all of the b_g are positive and each is a continuous function of temperature. If $\partial\Pi/\partial x = \infty$ for some x (for the TLU method this occurs when $x = 1.9$ or $x = 12$), then all b_g are positive but b_g is a discontinuous function of temperature.

If $\partial\Pi/\partial x = -\infty$ for some x, as it does for the RPF method at $x = 10^{-3}$, then the b_g near the discontinuity may be negative; it will also be a discontinuous function of temperature. To avoid negative b_g, the RPF method selects the equation used to evaluate Π based only on the value of x_{g+1}, see Eq. (48). The resulting b_g are still discontinuous functions of temperature as x_{g+1} crosses 10^{-3}. In addition, the RPF equation-selection technique results in inaccurate values near $x_{g+1} = 10^{-3}$ because the equation that is accurate for large-x is sometimes used to calculate $\Pi(x)$ for $x \ll 10^{-3}$ as well.

To reiterate, the b_g calculated using PB methods are always positive, continuous functions of temperature because $\partial\Pi/\partial x$ is finite.

An additional accuracy consideration is the error in the derivatives of the Planck spectrum with respect to temperature. The only methods that compute the first derivative of the Planck spectrum are the PB and the RPF methods. Both methods use Eq. (27) to relate the Planck and Rosseland integrals; therefore, the additional computational effort is small and no errors are introduced.

The results of the accuracy study are summarized rather simply. All of the

methods except MTR produce b_g that are accurate to within 2.5×10^{-3} relative error. If more accuracy is needed or desired, only PB methods allow that option. The TLU and RPF methods have the undesirable property that the calculated b_g are not continuous functions of temperature.

C. *Computing Speed*

Table I summarizes the accuracy and computing speed results of the several methods tested. The computing time results are obtained by repeatedly calculating b_g for the test problem while the CPU time is being accumulated. The CPU-time data in Table I are obtained by dividing the total CPU time by the number of repetitions, the number of groups, and the number of zones; this value is the CPU per result.

On a vector machine, such as the CRAY-X/MP48, the computing time depends upon the type of vectorization that is used. Therefore, for vectorized methods there are two values for the CPU time per result in Table I. The first value is for vectorization by group, e.g., the group index is incremented in the inner loop. In that case, Π is calculated once for each multigroup boundary, x_g. The second value in each CPU-time pair is for vectorization by zone. In the second case, Π must be calculated twice for most x_g. From the results in Table I, it is clear that group-wise vectorization is always preferable to zone-wise vectorization from a computing speed point-of-view. However, zone-wise vectorization may be necessary due to externally imposed constraints.

All of the approximate methods are faster than the numerical integration using the Newton–Cotes method; this is not surprising since the NC7 results are only used as a benchmark. The TLU method is about 6 times slower than the PB ($\Gamma_{9,3}$) and RPF methods with about the same accuracy. The MTR method is about 2 times faster than the PB and RPF methods; however, MTR is probably too inaccurate and unreliable for most applications.

From a combined accuracy and computing-speed point of view, the PB and RPF methods are the strong contenders. Table I shows that group-wise vectorization of the calculations is always faster than zone-wise vectorization. Therefore, the fastest and most-accurate results are obtained using the PB methods that have been vectorized by frequency group.

If external constraints require zone-wise vectorization (e.g., if the integrals can only be stored for one group at a time), then both the RPF and PB methods are available. The RPF method is about 5% faster than a comparably accurate PB method ($\Gamma_{9,3}$). However, for most uses 0.2% accuracy is not sufficient. In that case, a 35% speed penalty yields 3 orders of magnitude reduction in the maximum error for $\Gamma_{17,5}$. In addition, the results produced by the PB methods are positive and continuous functions of temperature, properties that are not guaranteed by the RPF method.

The third column of data in Table I shows the time required to calculate both spectra: Planck and Rosseland. For the RPF method, the additional time required to calculate the Rosseland spectrum is only 20% of the time to calculate the Planck

spectrum. For the PB methods, $\Gamma_{9,3}$, $\Gamma_{17,5}$, and $\Gamma_{21,10}$, The Rosseland penalties are 18%, 15%, and 8%, respectively.

For the combined calculation, the speed and accuracy guidelines are unchanged. It is always faster to use group-wise vectorization. A comparably accurate PB

V. Conclusions

A general method for calculating multigroup Planck and Rosseland integrals has been derived, tested, and compared with existing methods. The polylogarithm-based methods can be tailored to meet any accuracy requirements. Some versions of the PB methods are ten times faster than existing unvectorized methods such as TLU. The MTR method is faster than the PB methods, but it is not accurate enough for most applications.

The PB and RPF methods have the best combination of accuracy and computing speed. However, the RPF method is constrained to an accuracy of 0.2% which is inadequate for some applications. The RPF method also suffers from the problem that the integrals that are calculated are discontinuous functions of temperature. Group-wise vectorization of the PB methods is faster and more accurate than the RPF method. If zone-wise vectorization is necessary, the $\Gamma_{9,3}$ PB method is more accurate, positive, and continuous; the time penalty is only 5%.

When better accuracy is required, PB methods offer the only efficient alternative. For 35% time penalty, errors are reduced below 1.2×10^{-6}. For a 76% time penalty, the maximum error is reduced to 3.5×10^{-10}. The PB methods produce Rosseland integrals with a small (10–15%) penalty and produce a consistent multigroup cumulative probability distribution for use in Monte Carlo sampling of photon distributions.

Acknowledgments

This work was performed under the auspices of the U.S. Department of Energy.

References

1. G. C. Pomraning, *The Equations of Radiation Hydrodynamics* (Pergamon, New York, 1973).
2. L. Lewin, *Polylogarithms and Associated Functions* (Elsevier–North-Holland, New York, 1981).
3. K. S. Kölbig, J. A. Mignaco, and E. Remiddi, *BIT* **10**, 38 (1970).
4. I. S. Gradshteyn and I. M. Ryzhik, *Table of Integrals, Series, and Products*, 4th ed. (Academic Press, New York, 1965).
5. E. E. Lewis and W. F. Miller, Jr., *Computational Methods of Neutron Transport* (Wiley, New York, 1984).
6. G. Zimmerman, Private communication, 1986.